WAPD-T-3055

Stress Corrosion Cracking Behavior of Alloy 600 in High Temperature Water

G. L. Webb and M. G. Burke

To be Presented at Seventh International Symposium on Environmental Degradation of Materials in Nuclear Power Systems - Water Reactors
Breckenridge, CO, August 6-10, 1995

DOE Contract DE-AC11-93PN38195

BETTIS LABORATORY PITTSBURGH, PENNSYLVANIA 15122-0079

Operated for the U.S. Department of Energy
by WESTINGHOUSE ELECTRIC CORPORATION

DISCLAIMER

Conf-950816--2

Stress Corrosion Cracking Behavior of Alloy 600 in High Temperature Water

G. L. Webb and M. G. Burke
Westinghouse Electric Corporation
Bettis Laboratory
PO Box 79
West Mifflin, PA 15122-0079

Abstract

The stress corrosion cracking (SCC) susceptibility of Alloy 600 in deaerated water at 360°C, as measured with statically loaded U-bend specimens, is dependent upon microstructure and whether the material was cold-worked and annealed (CWA) or hot-worked and annealed (HWA). All cracking was intergranular, and materials lacking grain boundary carbides were most susceptible to SCC initiation. CWA tubing materials are more susceptible to SCC initiation than HWA ring-rolled forging materials with similar microstructures, as determined by light optical metallography (LOM). In CWA tubing materials, one crack dominated and grew to a size that was observable by visual inspection. HWA materials with a low hot-working finishing temperature (below 925°C) and final anneals at temperatures ranging from 1010°C to 1065°C developed both large cracks, similar to those found in CWA materials, and also small intergranular *microcracks*, which are detectable only by destructive metallographic examination. HWA materials with a high hot-working finishing temperature (above 980°C) and a high-temperature final anneal (above 1040°C), with grain boundaries that are fully decorated, developed only microcracks, which were observed in all specimens examined. These materials did not develop large, visually detectable cracks, even after more than 300 weeks exposure. A low-temperature thermal treatment (610°C for 7h), which reduces or eliminates SCC in Alloy 600, did not eliminate microcrack formation in the high temperature processed HWA materials. Detailed microstructural characterization using conventional metallographic and analytical electron microscopy (AEM) techniques was performed on selected materials to identify the factors responsible for the observed differences in cracking behavior. The major difference between the high-temperature HWA material and the low-temperature HWA and CWA materials was that the high temperature processing and final annealing treatment produced predominantly "semi-continuous" dendritic M_7C_3 carbides along grain boundaries with a minimal amount of intragranular carbides. Lower temperature processing produced significant proportions of intragranular M_7C_3 carbides, with less intergranular M_7C_3.

Introduction

Alloy 600 is susceptible to SCC in deaerated aqueous environments, most noticeably at temperatures above 316°C. SCC of Alloy 600 has been studied extensively since the observation of cracking in laboratory tests by Coriou[1], and there is a vast amount of literature on the effect of environment, material condition, temperature, and stress on SCC initiation[1-4]. Previous SCC initiation test data[5] from two very susceptible heats of tubing showed a temperature dependence corresponding to an activation energy of 50.6 kcal/mole, and a stress dependence of $\sigma^{5.7}$. Previous studies showed that SCC susceptibility in Alloy 600 is related to the intergranular precipitation of Cr-rich carbides[2-4]. The formation of a "continuous" intergranular carbide network is associated with good SCC performance in a deaerated water environment, whereas materials with "clean" grain boundaries, or those which have few carbides, are more susceptible to SCC. The differentiation between "good" and "poor" microstructures does not depend on the extent or presence of a Cr-depleted zone near the intergranular carbides, particularly as the more resistant microstructures generally exhibit more pronounced Cr-depletion[6]. Furthermore, materials that receive a low-temperature thermal treatment at 610°C, which promotes grain boundary Cr-depletion, are more resistant to SCC, although very little change in microstructure may be observed by LOM examination.

Studies were conducted in high temperature deaerated water to determine if the working method, ring forging and annealing vs. cold drawing and annealing, had an effect on SCC initiation. At the completion of SCC testing of the ring forged materials, three ring forgings from two heats, with both high and low finishing temperatures, were selected for examination by AEM to attempt to determine the microstructural characteristics that could lead to the observed SCC differences between these two materials.

Test Materials

CWA tubing materials came from more than 40 heats of Alloy 600 tubing with an outer diameter (OD) of 12.7 or 14.3 mm and a minimum wall thickness of 1.07 mm or 1.35 mm, respectively. The tubing heats have carbon con-

tents between 0.02% and 0.05%[a]. The tubing was produced by a normal tube reduction process. In this process, the final operations were tube sinking with more than 50% reduction, final annealing in hydrogen while traveling through the hot zone of a furnace where the material was at temperature for several minutes, rotary straightening, and belt polishing of the OD surface. Tubing from heat A, the most susceptible tubing heat tested[5], which has between 10% and 50% grain boundary decoration (GBD) with carbides as estimated from LOM examination, had been final-annealed at a temperature of 925°C, while all other heats of tubing were annealed at temperatures between 1010°C and 1093°C to achieve a microstructure with carbide-decorated grain boundaries. High final annealing temperatures, which put more carbides into solution, result in more GBD than low final annealing temperatures. The amount of GBD is very dependent on the cooling rate from the final anneal, and for thin-wall tubing it is easy to have a cooling rate that is fast enough to leave carbon in solution, resulting in a less desirable microstructure.

In addition to the tests conducted on CWA tubing, SCC tests were also conducted on specimens from 59 ring forgings from 10 heats of material. The carbon contents for all the ring forging heats varied from 0.03% to 0.06%. Ring forging is a three step process, starting with a 25 cm diameter billet reduced from a 50 cm diameter ingot. The billet was upset forged to produce a "pancake" from a temperature of 1150°C. A hole was punched in the pancake, which was then given an intermediate ring roll, starting at a temperature of 1150°C and finishing at about 925°C. Final ring rolling was done at a starting temperature of 1150°C and finishing at about 925°C. The finished ring forging had a 71 cm outside diameter and a 5 cm ring thickness. Final annealing occurred in the 1010-1065°C temperature range, with a cooling rate that was controlled at 220 C-deg per hour to a temperature of 650°C, followed by air cooling. The final annealing temperature was selected, based on trial anneals, to produce carbide-decorated grain boundaries while maintaining the room temperature yield strength above 204 MPa.

As-processed Alloy 600 has a tendency to develop "*bands*" that consist of fine-grained regions containing many intragranular carbides. "Banding" is discussed in more detail in the Results Section. Optimizing the thermo-mechanical processing of Alloy 600 ring forgings by employing high-temperature processing treatments (completing ring rolling above 980°C with 28% final rolling reduction) tends to minimize the banded microstructure, as opposed to the low-temperature processing (completing ring rolling at 925°C or below). The effect of ring rolling finishing temperature on the SCC susceptibility was included as a variable in this program. The processing parameters for the three ring forgings selected for the AEM examination are listed in Table 1.

Experimental Procedures

SCC Testing

Specimen types included split tubing U-bends (STUBs) tested with the inside diameter (ID) surface in tension, double U-bends (DUBs), and a small number of single U-bends (SUBs). STUBs were used to test CWA tubing materials, and DUBs and SUBs were used to test HWA ring forging materials. The ID surface of tubing was as-annealed in hydrogen, with no additional machining operations, and the ID surface is $< 1.6\ \mu m$ (RMS) following tubing manufacture. Double U-bend and single U-bend specimens had a machined surface with a finish of $< 3\ \mu m$ (RMS).

SCC tests were conducted in a stainless steel autoclave at a temperature of 360°C. The SCC test environment was flowing (1-2 cc/s), deaerated, pressurized water ($\approx$10 ppb dissolved O_2) with a pH of 10.1-10.3 at room temperature and a hydrogen concentration of 10-60 cc (STP) H_2/kg H_2O at a pressure of $\approx$ 20 MPa. Specimens were removed from the autoclave periodically for visual inspections at a magnification of 30X, and uncracked specimens were returned to the autoclave for further exposure.

Light Optical Metallography

Specimens for microstructural examination were prepared using conventional metallographic preparation techniques, followed by electrolytic etching with 8:1 orthophosphoric acid to water. The degree of grain boundary carbide coverage was estimated from photomicrographs taken at 500X.

---

[a] All compositions are in weight percent.

Analytical Electron Microscopy

Three ring forgings were selected for detailed microstructural examination. Two ring forgings from the same heat (Heat B), but with high or low temperature processing, were selected to investigate the effect of processing treatment while eliminating heat-to-heat effects. A third ring forging (Heat C), with low temperature processing but a higher temperature final anneal that was close to the final annealing temperature of the high temperature processed ring forging, was selected to investigate the effect of final annealing treatment.

Both thin-foil and carbon extraction replica specimens were obtained from the two Heat B ring forgings. For comparison, AEM specimens were also prepared from the Heat C ring forging. Electron-transparent thin-foil specimens were prepared using conventional electropolishing techniques with an electrolyte of 20% $HClO_4$ - 80% CH_3OH at ≈-40°C. The extraction replica specimens were prepared using a solution of 5% Br in CH_3OH. Microstructural characterization was performed using a Philips CM12 and a Philips EM420 analytical electron microscope operated at 120kV and equipped with Link Analytical ultra-thin window energy dispersive x-ray spectrometers (EDS). Precipitates were identified by electron diffraction techniques and microchemical analysis using the scanning transmission electron microscopy (STEM) mode of the AEM. STEM-EDS x-ray maps were obtained from the carbon extraction replica specimens to complement the thin-foil analyses.

Results

SCC Test Results

The SCC data were separated into two major groups based on the working treatment that the base material received, either hot work or cold work. Within each of these groups, the data were grouped based on the amount of grain boundary carbide decoration. The groupings correspond to 10-50%, 50-75%, 75-90%, and 90-100% decoration. Cumulative failure[b] plots were made of the SCC data using the procedure described by Nelson[7]. Previous results[5] indicated that the failure times were distributed lognormally (i.e., the logarithms of the failure times are normally distributed). The data are characterized by two parameters, the median failure time, which is the intercept at 50% failures, and the slope of the curve, which is a graphical estimate of the standard deviation.

The raw SCC data separate into groups that are statistically different and consistent with the degree of grain boundary carbide decoration, indicating that the observed SCC behavior is dependent on the microstructure. Tubing and ring-forging materials have different yield strengths, resulting in different initial stresses being imposed by the constant deflection U-bend specimens. Because stress has such a strong effect on SCC initiation, it is necessary to account for this effect in the initiation data to determine the true effect of material condition on SCC initiation. Strain measurements on STUBs and DUBs indicate (true) plastic strains of 18% and 14%, respectively. Stresses were calculated for the various groups of materials tested using a power law mathematical approximation of a true stress-true strain curve developed from multiple heats of Alloy 600. In this approximation, the power law exponent, n, is a function of the yield strength, σ_y.

$$\sigma = 1535\ (\ 0.0185 + \epsilon_p\ )^n$$

$$n = 0.256 \ln\left(\frac{1535}{\sigma_y}\right)$$

where n = *strain hardening exponent,*
ϵ_p = *plastic (true) strain, and*
σ_y = *yield strength (MPa)*

The SCC test data, normalized to a common applied stress, are shown in Figure 1. All the SCC test data were normalized to a common test stress of 815 MPa, which is the stress determined for the STUB specimens taken from tubing from Heat A[5]. Estimates of the as-tested stresses on the various groups of specimens (i.e., ring forgings, tubing) were made based on the yield strength of the material and the measured specimen strain. A yield strength of 204 MPa, which is consistent with the yield strength values measured for these materials, was used for determining stresses in all materials that were annealed at > 1010°C. These estimated stresses are about 580 MPa for ring forging DUB specimens and 680 MPa for STUB specimens. The failure times were adjusted by using the previously determined stress exponent for SCC initiation of -5.7. For example, the failure times for ring forging DUB specimens were reduced by a factor of $(815/580)^{5.7} \approx 7$. No failures were observed in tubing with 90-100% grain boundary decoration, although tests were discontinued after a short time (42 weeks), or in ring forging

[b] Based on visual observation of SCC initiation at 30X magnification.

material with > 90% grain boundary decoration after 300 weeks. These data are indicated by arrows in the figure. All of the failures in HWA material, regardless of the degree of grain boundary decoration, occurred in the material that was final annealed at between 1010° and 1040°C.

The results plotted in Figure 1 show that there is a difference in SCC susceptibility between CWA and HWA materials, even after normalizing for the differences in stresses between the materials and specimen types. For a given microstructure and stress, HWA materials are more resistant to SCC initiation than CWA materials.

Destructive Examination Results

Destructive examinations (DE) were undertaken on some of the DUB specimens from ring forgings to determine if small cracks were occurring that were not visible during the normal visual examinations. Based on extensive previous experience with testing of STUB specimens of tubing, no small cracks were anticipated. Specimens were selected at random from those remaining in test at the completion of 255, 273, and 296 weeks. The specimens were sectioned longitudinally and mounted so that both an edge and centerline could be examined in the as-polished condition at a magnification of 200X or greater. When many small cracks of a uniform size were found, especially in the high temperature processed ring forging materials, they were called microcracks to differentiate them from the large cracks detectable by 30X visual examination. A typical microcrack is shown in Figure 2.

The DE results are shown in Table 2. Forty-one ring forging specimens with low-temperature processing were randomly selected for DE, and a majority (31) did not have microcracks. Thirteen ring forging specimens with high-temperature processing were randomly selected for DE, and all had at least one microcrack, although a scanning electron microscope (SEM) examination was required to find cracks on one specimen. In contrast, no microcracks were found during an SEM examination of an uncracked low-temperature processed specimen. The final group of specimens selected for DE also included specimens that had received a low-temperature thermal treatment at 610°C for 7h, and three of these six specimens had microcracks.

Light Optical Microstructural Characterization Results

The grain size of the high-temperature processed forging material sample, final-annealed at 1060°C for 2h, was approximately 200 μm, as compared to the $\approx$100 μm grain size of the low-temperature processed forging Heat B sample that was final-annealed for 1h at 1024°C. The low-temperature processed forging material from Heat C, which received a final anneal at 1050°C for 2h, also had an average grain size of $\approx$100 μm. The yield strengths for these three material conditions, although not strictly related to the grain size and microstructure, were significantly different and are listed in Table 1. The general microstructure of these materials is presented in Figure 3.

Examination of the metallographic specimens from the low-temperature processed materials revealed the presence of a duplex grain structure, with many intragranular carbides (most likely MC-type inclusions) associated with the fine-grained regions or bands. Ring forgings frequently develop patterns of banding, obvious in metallographic mounts and low magnification photomicrographs, Figure 4, with dark-appearing regions containing extensive, coarse, intragranular carbides and little intergranular precipitation, alternating with light-appearing regions with no intragranular precipitation and significant amounts of intergranular precipitation.

Analytical Electron Microscope Characterization Results

The results of the AEM evaluation are summarized in Table 3, and are described in the following sections.

Heat B - High Temperature Processing

The high-temperature processed Heat B ring forging, with a carbon content of 0.042%, was final-annealed at 1060°C for 2h. The LOM metallographic evaluation showed nearly complete grain boundary carbide decoration (>90% GBD), with a very small amount of intragranular carbide precipitation. AEM characterization of this material revealed extensive intergranular Cr-rich M_7C_3 carbides, Figure 5, with about 85% GBD. These carbides generally appeared in thin-foil specimens as "semi-continuous" precipitates, $\approx$0.2 μm in thickness and varying in length up to $\approx$7 μm. Several fine, discrete $M_{23}C_6$ carbides were also observed at some boundaries, Figure 6. More detailed examination revealed that the morphology of the intergranular M_7C_3 was a complex dendritic type, Figure 7. These secondary electron images were obtained from an inclined grain boundary region after a light electrolytic etch that shows the 3-dimensional morphology of the intergranular M_7C_3. Although the predominant carbide configuration was intergranular, isolated regions contained a high proportion of intragranular M_7C_3 carbides that

may be due to incomplete removal of carbide banding. An example of such a region with both the intergranular and intragranular carbides is shown in Figure 8.

Heat B - Low Temperature Processing

The low-temperature processed Heat B ring forging was final-annealed at 1024°C for 1h. The LOM metallographic evaluation indicated about 50-75% GBD, which is typical for ring forgings annealed at this temperature, whereas the AEM analysis indicated about 50-60% GBD. Intergranular M_7C_3 and $M_{23}C_6$ were observed at many high-angle grain boundaries, Figure 9. The coarse intergranular M_7C_3 had a dendritic morphology similar to that observed in the 1060°C specimens from Heat B. The $M_{23}C_6$ were discrete intergranular carbides, approximately 0.1 μm in length.

STEM-EDS x-ray maps confirmed that the majority of the carbides are Cr-rich. However, a few Ni-rich precipitates, frequently associated with the Cr-rich carbides, were also detected. The x-ray maps, Figure 10, indicate that a central portion of the carbide is Ni-rich. Electron diffraction confirmed that these precipitates had a face centered cubic (fcc) structure, with a lattice parameter $\approx$3 times that of the matrix, and exhibited a cube-cube orientation relationship with the matrix. Such Ni-rich intergranular precipitates have been observed in other studies of NiCrFe alloys[8,10], and have been identified as $Ni_{23}(B,C)_6$. The electron diffraction and STEM-EDS data indicate that the fine precipitates in the ring-forged specimens are Ni-rich $M_{23}X_6$, where X represents B and C.

This material was also characterized by extensive intragranular M_7C_3 precipitation. Two carbide morphologies were observed for the intragranular precipitates: globular and facetted, Figure 11. Examination of the facetted carbides indicates that there are multiple habit planes with the matrix, and the crystallographic morphology suggests that this carbide formed upon cooling from the final anneal temperature. The globular M_7C_3 precipitates appear to have formed during prior thermo-mechanical processing, and were not fully dissolved during the final anneal. Both intergranular and intragranular carbide morphologies are shown in the SEM micrographs of Figure 12.

Heat C - Low Temperature Processing

The low-temperature processed Heat C ring forging, with a carbon content of 0.052%, was final-annealed at 1050°C for 2h. The LOM evaluation indicated 50-75% GBD, similar to the Heat B forging annealed at 1024°C for 1h. Ring forgings that were final-annealed at 1050°C had either 50-75% or 75-90% GBD. The grain sizes of these two materials were also comparable ($\approx$100 μm). The estimated grain boundary coverage from AEM examination is 50-60%. The AEM examination revealed a microstructure with extensive regions of intragranular M_7C_3 carbides, coarse globular-type M_7C_3 intergranular carbides, and fine intergranular $M_{23}C_6$ carbides. Examples of the various carbides are presented in Figure 13. Although this material exhibited a similar extent of intergranular carbide precipitation to that observed in the Heat B ring forging final-annealed at 1024°C for 1h, no semi-continuous or dendritic-type M_7C_3 carbides were detected. The discrete globular M_7C_3 morphology may be related to the cooling rate from the forging and final annealing temperatures.

Discussion

The SCC susceptibility of Alloy 600 has been correlated with the optical microstructure as determined with the 8:1 orthophosphoric acid electrolytic etch, which primarily attacks chromium-containing precipitates. Materials that do not have a high proportion of intergranular chromium carbides are more susceptible to cracking than materials with highly decorated grain boundaries[2,4]. The AEM examination indicated that the microstructures with the highest resistance to SCC initiation had a high amount of intergranular M_7C_3 precipitates, which precipitated during cooling from the high-temperature final anneal.

The degree of grain boundary carbide decoration in HWA materials did not correlate completely with the final annealing temperature. Materials annealed between 1010°C and 1040°C developed either 50-75% or 75-90% decoration, but the materials with the higher grain boundary decoration were more resistant to SCC initiation. No cracks initiated in HWA materials that were final annealed above 1040°C, even though some had < 75% grain boundary decoration.

This study also found that the SCC susceptibility of Alloy 600 is dependent upon how the material was processed, whether by cold-work and annealing or hot-work and annealing, and upon the hot-working parameters, especially the working temperature. CWA tubing materials were found to be more susceptible to SCC initiation than HWA ring forging materials with similar LOM microstructures. Even when corrected for differences in the as-tested

stress levels, CWA materials are more susceptible to SCC initiation, with the differences being statistically significant at the 95% confidence level. When corrected for strength differences, the HWA materials with 50-75% GBD have failure times that are a factor of 5 longer than the failure times for CWA tubing materials.

The difference is not believed to be due to differences in stress relaxation between the two specimens types, STUB vs. DUB or to residual stress differences. The STUB specimens have a higher measured strain than the DUB specimens, and at the same yield strength levels, the STUB specimens will have a higher stress. Stress relaxation would be expected to be higher in the more highly strained specimens, resulting in longer crack initiation times for the STUB specimens, but the difference in failure times is in the opposite direction. Stress relaxation would have to be about 34% higher in the lower stressed DUB specimen than in the STUB specimen to account for the difference in SCC initiation times. Residual stresses would not be responsible for the differences in SCC susceptibility. Although the machined surfaces of double U-bend specimens will have higher residual stresses than the final annealed surfaces of tubing specimens, the high strains imposed during bending, 14-18%, will minimize this effect because the strain associated with a 300 MPa residual stress is only 0.15%.

There are two significant differences between the processing of hot-worked forging materials and cold worked tubing materials, other than the obvious differences in working temperature. First, the microstructural results may be misleading. The tubing materials have very thin walls, less than 1.2 mm, and cooling rates that are too fast to allow for carbide precipitation are easily achieved. The orthophosphoric acid etch attacks both the carbides and the matrix near the carbides, so the presence of unprecipitated carbon at the grain boundary could also contribute to the grain boundary decoration in the LOM microstructure. Previous work has shown that the low temperature thermal treatment at 610°C is beneficial in improving the SCC resistance of Alloy 600 tubing, and has the greatest effect in materials with the poorest microstructures, with less visible grain boundary carbide precipitation[5]. Because of the low temperature involved in this thermal treatment, no significant amount of diffusion occurs, so only the carbon already present at the grain boundary is given a chance to precipitate during this thermal treatment. This results in an improvment in the SCC resistance, sometimes without a significant change in the LOM microstructure. In the forging rings, which have a heavier section size and a slower cooling rate, carbides have a greater opportunity to precipitate during cooling from the final anneal, and the bulk of the grain boundary decoration comes from actual precipitates rather than from supersaturated carbon in solution at the grain boundary.

The second major difference between tubing and ring forgings is in the final annealing atmosphere. Tubing is final annealed in a dry hydrogen atmosphere, and the final tested surface is the as-hydrogen-annealed surface, whereas forgings are final annealed in an inert atmosphere, but the tested surface is machined. It can be inferred from two other phenomena, which show that hydrogen has a detrimental effect on SCC, that final hydrogen annealing may be detrimental to SCC resistance. First, Airey[11] indicated that SCC initiation times were much longer for specimens tested in an autoclave containing pure water without a hydrogen overpressure than with a hydrogen overpressure. The presence of an oxide film on the surface also affected the SCC resistance by interfering with the hydrogen transport to the metal. Second, pickling, which introduces hydrogen into the metal, has a detrimental effect on the SCC resistance of Alloy 600[2]. The difference in the susceptibility to SCC initiation between the CWA tubing and HWA ring forgings is attributed mainly to the hydrogen final-annealing atmosphere used in tubing manufacture.

In addition to the differences between CWA and HWA materials in the initiation of visually detectable SCC, a phenomenon called ***microcracking*** was observed in HWA materials. Microcracks are shallow intergranular cracks, typically on the order 125 μm in depth. HWA materials that were processed at temperatures below 925°C developed both large cracks and microcracks, but HWA materials from 3 heats (35 forgings), which were processed at temperatures above 980°C to eliminate banding, developed only microcracks. No microcracking has been observed in specimens from CWA tubing materials, including specimens that were destructively examined following completion of long term testing (as much as 500 weeks at 288°C) of tubing materials that were previously reported[5].

The processing of ring forgings was investigated to find a way to eliminate banding. When the major part of the hot-working operation was completed above the carbide solvus temperature ($\approx$ 1030°C for 0.040% carbon[8]) and when the annealing treatments were carried out at temperatures about 15 - 40 C-deg above the carbide solvus, the banding was minimized or eliminated. On the other hand, when hot-working and annealing took place considerably below the carbide solvus temperature, such as below 925°C, or when the annealed material is slowly cooled through the carbide precipitation region, the banding occurred or reoccurred depending on the material's tendency toward banding.

Banding is a concern because the microstructure within the dark bands contains little of the intergranular Cr-rich carbide precipitates necessary for SCC resistance. Elimination of banding is desirable for reducing the susceptibility to SCC initiation since it has provided an initiation site for SCC. Once bands form, they are persistent, remaining even after high-temperature reannealing. Electron microprobe examination indicated that these dark bands are regions with enrichments of Cr, Mn, and Ti, and depletion of Fe, which occur during solidification. The preferential intragranular carbide precipitation within these bands is consistent with the affinity of C for Cr and Ti. The persistence of the bands, despite attempts at eliminating them by reannealing, is due to the sluggish diffusion rates of Cr, Mn, and Ti. High-temperature annealing, above the carbide solvus, will homogenize the interstitial carbon in solution, but not the substitutional elements, and slow cooling through the carbide precipitation range allows the bands to re-form during cooling. Later studies, which focused on using high-temperature processing to encourage homogenization of the Cr, Mn, and Ti-enriched regions, resulted in microstructures with significantly reduced banding. This high-temperature processing was utilized only on ring forgings from 3 heats of material.

As anticipated, based on the LOM microstructures with fully decorated grain boundaries, the specimens from these high-temperature processed ring forgings did not develop visually detectable cracks during testing. A destructive metallographic examination of selected specimens indicated very shallow intergranular cracking, not detectable by 30X visual inspections. These materials developed either single or multiple (up to 10 have been observed) microcracks.

The occurrence of microcracking is not related to only the temperature of the final anneal; low-temperature processed HWA materials with final anneals of 1065°C did not develop microcracks to the same extent as the high-temperature processed HWA materials with lower final annealing temperatures. Microcracking has thus far been the only form of SCC observed in high-temperature processed and high-temperature annealed ring forgings.

Based on pre-test examinations of several specimens, these microcracks do not form during bending, but require exposure to the environment to initiate. The exposure time required for the initiation has not been determined, but only specimens with exposures longer than 250 weeks were examined for microcracks. Likewise, the growth rate of microcracks has not been determined, but it appears to be slow, with no obvious changes in number or depth of cracks in specimens examined at 250 or 300 weeks. A low-temperature thermal treatment (610°C for 7h) has been found to greatly reduce or eliminate SCC in both CWA and HWA with low hot-working finishing temperatures. However, microcracks were observed in three of six low-temperature thermally-treated specimens from HWA materials with a high hot-working finishing temperature.

It is not clear whether microcracking is the same as SCC, or a different phenomenon. Microcracks are intergranular, occur after exposure to water, and occur in a material that is susceptible to SCC. If microcracking is the same as SCC, its presence depends on a slow crack growth rate. Since the formation of a large crack will relieve stresses at the tensile surface of the specimen, so that other cracks will not be likely to form, multiple cracks may have a chance to form in materials that do not quickly develop a large crack. Microcrack formation may be a different phenomenon than SCC. The conventional wisdom with SCC is that high-temperature annealing and slow cooling, which produce grain boundaries with abundant chromium carbide precipitation, result in a material that is more resistant to SCC formation. This is clearly not the case for microcracks, for they formed in 100% of the high-temperature processed HWA materials, which have the most completely decorated grain boundaries. There may be a relationship between the Cr-carbide morphology and the susceptibility to microcracking. In the high-temperature processed ring forgings, most susceptible to microcracking, the predominant Cr-carbide is M_7C_3 with a dendritic morphology. In the low-temperature processed ring forgings, which are less susceptible to microcracking, both globular and dendritic M_7C_3 were observed.

The SCC mechanism in Alloy 600 has not been unequivocally established, and at least 5 different mechanisms are under consideration (dissolution-oxidation, hydrogen embrittlement, corrosion-enhanced plasticity, creep, and internal oxidation). Therefore, with microcracks observed only in statically loaded specimens from hot-worked and annealed materials after long term exposures to a single high temperature water environment, it is difficult to ascertain whether the same mechanism is responsible for SCC and microcracking.

Microcrack formation is a problem, even though it has not been detected under normal SCC testing procedures where visual examinations at 30X are utilized to detect cracking. Under conditions involving cyclic loading, these microcracks may result in a degradation in the environmentally assisted cracking behavior because of the presence of a sharp crack tip. The strain levels required to induce microcracking have not been determined, and thus far they have been observed in DUB with 14% strain. If microcracks develop in Alloy 600 at strain levels of $< 5\%$, which

can be induced in wrought Alloy 600 as a result of weld shrinkage, the results from statically loaded specimens would not conservatively predict the behavior of actively loaded structures.

The AEM microstructural characterization confirms that the presence of intergranular carbides enhances the resistance of the material to the formation of large SCC cracks. In the material most resistant to the initiation of large cracks, high-temperature processed Heat B, these carbides are Cr-rich M_7C_3 with a dendritic morphology. These carbides were also observed, although to a lesser degree, in the low-temperature processed Heat B ring forging. As indicated above, materials with this dendritic carbide morphology may have a greater tendency to microcrack formation.

Based on the microstructural examination of the 1024°C and 1060°C final anneal forgings, a high-temperature final anneal is essential for carbide dissolution. The two intragranular carbide morphologies suggest that other factors, such as banding, may be responsible for the increased proportion of intragranular carbide precipitation in the materials that were annealed at 1024°C.

The estimates of the degree of grain boundary carbide decoration are lower based on AEM examination than the estimates from the LOM because the orthophosphoric acid etchant attacks both the carbides and matrix near the carbides, thus yielding an overestimate of the proportion of grain boundary carbides. The AEM observations also serve to demonstrate that materials which appear to be very similar by optical metallographic analysis, such as the materials final-annealed at 1024°C and 1050°C, can exhibit pronounced microstructural differences in terms of extent and nature of carbide precipitation.

Conclusions

Material with a microstructure consisting of carbide-decorated grain boundaries is resistant to SCC initiation in high temperature deaerated water. This microstructure may be developed with a high-temperature final anneal which can dissolve the pre-existing carbides and promote extensive intergranular M_7C_3 precipitation upon cooling. The difference in susceptibilities of CWA and HWA Alloy 600 materials with similar LOM microstructures, however, is an indication that more sophisticated techniques are necessary to provide a true indication of SCC susceptibility.

CWA tubing materials are more susceptible to SCC initiation than HWA materials with microstructures that have similar degrees of grain boundary carbide decoration based on LOM examination. This difference remains even when yield strength differences between the materials are taken into account. The difference in susceptibilities is attributed to the hydrogen final-annealing atmosphere used in tubing manufacture, and to the effect of the thin wall of the tubing on carbide precipitation during cooling.

Although resistant to general SCC, HWA materials with high-temperature processing, which was used to eliminate the banded microstructure, have the greatest tendency to develop microcracks. The shallow microcracks that have been observed in these materials are associated with "good" microstructure, i.e., extensive precipitation of semi-continuous intergranular Cr-rich M_7C_3 carbides. In the high-temperature processed ring forgings, these carbides have a dendritic morphology. Despite the fact that these microcracks have not developed into visually detectable cracks in statically loaded specimens, their presence may lead to a degradation in SCC resistance if they also occur in actively loaded applications.

The estimates of the degree of grain boundary carbide decoration are lower based on AEM examination than the estimates from the LOM because the orthophosphoric acid etchant attacks both the carbides and matrix near the carbides, thus yielding an overestimate of the proportion of grain boundary carbides.

The AEM microstructural characterization confirms that the presence of intergranular carbides enhances the resistance of the material to the formation of large SCC cracks. In the material most resistant to the initiation of large cracks, high-temperature processed Heat B, these carbides are Cr-rich M_7C_3 with a dendritic morphology. These carbides were also observed, although to a lesser degree, in the low-temperature processed Heat B ring forging. Although no correlation has been established, materials with this dendritic carbide morphology may have a greater tendency to the formation of microcracks. Based on the microstructural examination of the ring forgings with either a 1024°C or 1060°C final anneal, a high-temperature final anneal is essential for carbide dissolution. The two intragranular carbide morphologies suggest that other factors, such as banding, may be responsible for the increased proportion of intragranular carbide precipitation in the materials that were annealed at 1024°C.

The AEM observations also serve to demonstrate that materials which appear to be very similar by optical metallographic analysis, such as the materials final-annealed at 1024°C and 1050°C, can exhibit pronounced microstructural differences in terms of extent and nature of carbide precipitation.

Acknowledgments

The technical assistance of J.J. Haugh of the Westinghouse Science & Technology Center and A.J. Falco of Bettis Laboratory for the preparation of AEM specimens is greatly appreciated. Dr. George J. Salvaggio, retired from Westinghouse, was responsible for the development of the analytical method for determining Alloy 600 stress-strain curves.

This work was performed under U.S. Department of Energy Contract DE-AC-93PN38195 with Bettis Laboratory, Westinghouse Electric Corporation.

References

1. H. Coriou, et al., "High Temperature Stress Corrosion Cracking of Inconel in Water", Third Metallurgical Symposium on Corrosion (Aqueous and Gaseous), 1959 (North Holland Publishing Co., Amsterdam, 1960) pp. 161-169.

2. D. Van Rooyen, "Review of the Stress Corrosion Cracking of Inconel 600", Corrosion 31, 1975, pp. 327-337

3. H. A. Domian, R. H. Emanuelson, L. Katz, L. W. Sarver, and G. J. Theus, "Effect of Microstructure on Stress Corrosion Cracking of Alloy 600 in High Purity Water", Corrosion 33, 1977, pp. 26-37

4. G. P. Airey, "The Effect of Carbon Content and Thermal Treatment on the Stress Corrosion Cracking Behavior of Inconel Alloy 600 Steam Generator Tubing", Paper 195 presented at NACE Corrosion/78 in March 1978 in Houston

5. G. L. Webb, "Environmental Degradation of Alloy 600 and Welded Filler Metal EN82 in an Elevated Temperature Aqueous Environment", Sixth International Symposium on Environmental Degradation of Materials in Nuclear Power Systems - Water Reactors, San Diego, CA, 1993 (TMS, Warrendale, PA), pp. 687-691

6. G. S. Was and V. B. Rajan, "The Mechanism of Intergranular Cracking of NiCrFe Alloys in Sodium Tetrathionate", Met. Trans. 18A, 1987, pp. 1313-1323

7. Wayne Nelson, ACCELERATED TESTING - Statistical Models, Test Plans, and Data Analyses, Wiley Series in Probability and Mathematical Statistics - Applied Probability and Statistics, John Wiley & Sons, New York, 1990.

8. R. C. Scarberry, S. C. Pearman, and J. R. Crum, "Precipitation Reactions in Inconel Alloy 600 and Their Effect on Corrosion Behavior", Corrosion 32, 1976, pp. 401-406

9. R. M. Kruger and G. S. Was, "The Influence of Boron on the Grain Boundary Chemistry and Microstructure of Ni - 16Cr - 9Fe - 0.03C", Met. Trans. 19A, 1988, pp. 2555-2566

10. K. Stiller, "Intergranular Precipitation in Ni-Cr-Fe Alloys", Surface Science 266, 1992, pp. 402-408

11. G. P. Airey, "The Stress Corrosion Cracking (SCC) Performance of Inconel Alloy 600 in Pure and Primary Water Environments", Proceedings of the International Symposium on Environmental Degradation of Materials in Nuclear Power Systems - Water Reactors, Myrtle Beach SC, 1983 (NACE, Houston, TX), pp. 462-476

Table 1: Summary of Processing, Grain Size, and Yield Strength for Alloy 600 Materials Referenced

Heat	Carbon, %	Ring Rolling Finishing Temperature	Final Anneal	Grain Size	Yield Strength
Heat A	0.04	N/A - CWA Tubing	925°C	20 μm	340 MPa
Heat B	0.041	High Temperature	1060°C	200 μm	175 MPa
Heat B	0.041	Low Temperature	1024°C	100 μm	204 MPa
Heat C	0.052	Low Temperature	1050°C	100 μm	230 MPa

Table 2: Results of Destructive Examination of Double U-Bend Ring Forging Specimens

Ring Forging Material Heat Treatment	No. Examined	No. with Microcracks
HWA with Low Temperature Processing	41	10
HWA with High Temperature Processing	13	12(†)
HWA with High Temperature Processing + LTTT(‡)	6	3

† A microcrack was observed in the "uncracked" specimen during SEM examination.
‡ Low-Temperature Thermal Treatment, 610°C for 7h

Table 3: Summary of AEM Results

Heat	Hot Work Finishing Temperature	Grain Boundary Decoration, % Visual	AEM	Comments
B 0.041% C	HWA High Temp + High Temp Anneal	90-100	85	Intergranular dendritic (semi-continuous) Cr-rich M_7C_3 Some fine intergranular $M_{23}C_6$ Few intragranular carbides
B 0.041% C	HWA Low Temp + Mid Temp Anneal	50-75	50-60	Intergranular coarse dendritic Cr-rich M_7C_3 Some discrete intergranular $M_{23}C_6$ & Ni-rich $M_{23}X_6$ Extensive intragranular globular and facetted M_7C_3 (Globular precipitate from prior processing)
C 0.052% C	HWA Low Temp + High Temp Anneal	50-75	50-60	Coarse globular intergranular M_7C_3 and fine intergranular $M_{23}C_6$ (No intergranular dendritic M_7C_3) Coarse intragranular M_7C_3

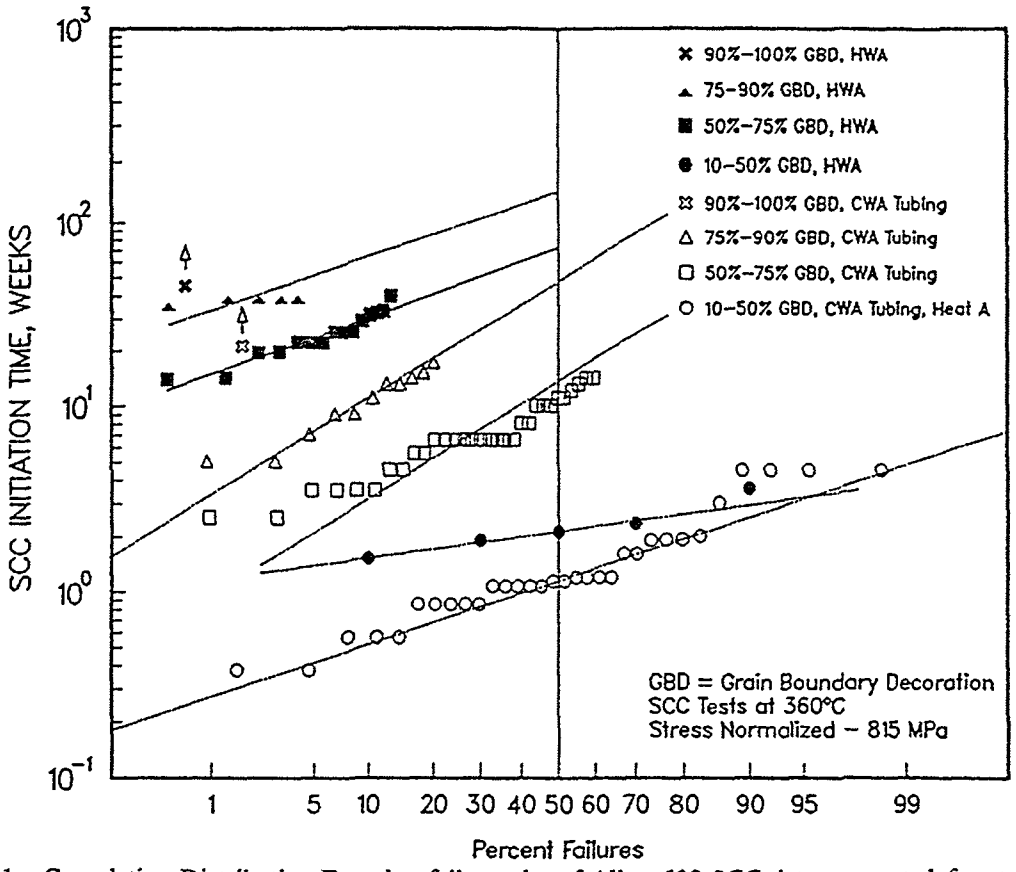

Figure 1: Cumulative Distribution Function failure plot of Alloy 600 SCC data, corrected for stress

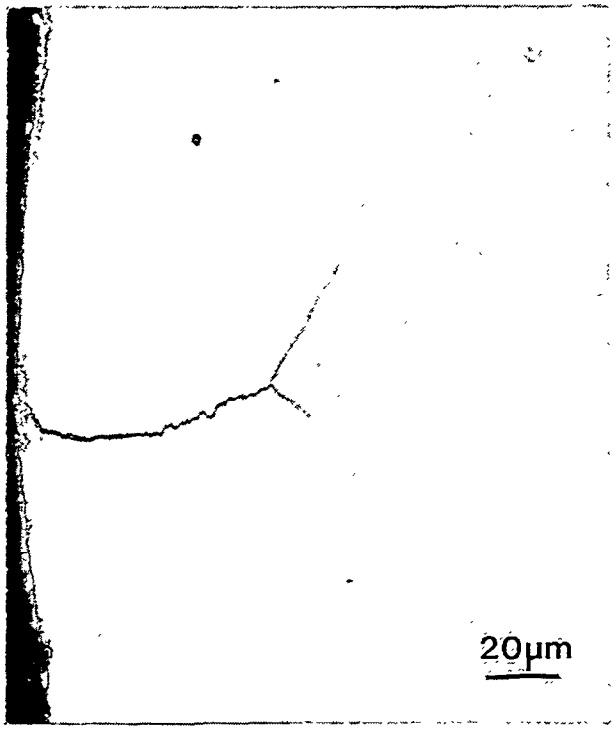

Figure 2(a): Microcrack in as-polished SCC specimen

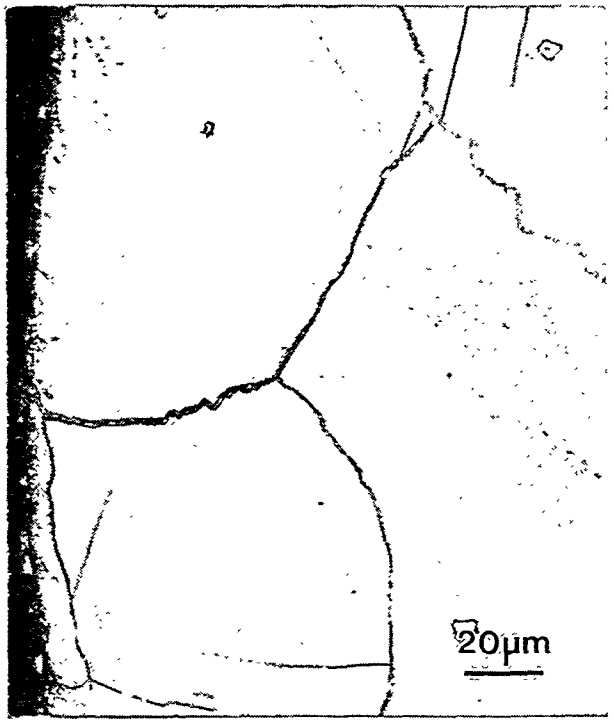

Figure 2(b): Microcrack in Orthophosphoric acid etched SCC specimen

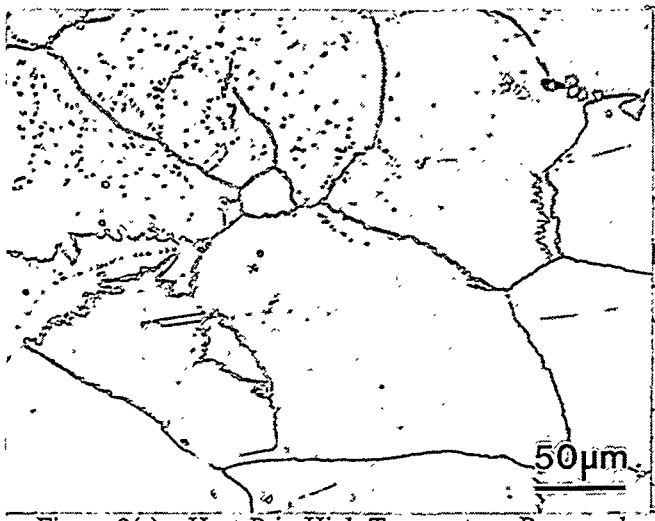

Figure 3(a): Heat B in High Temperature Processed Condition - Orthophosphoric Acid Etch

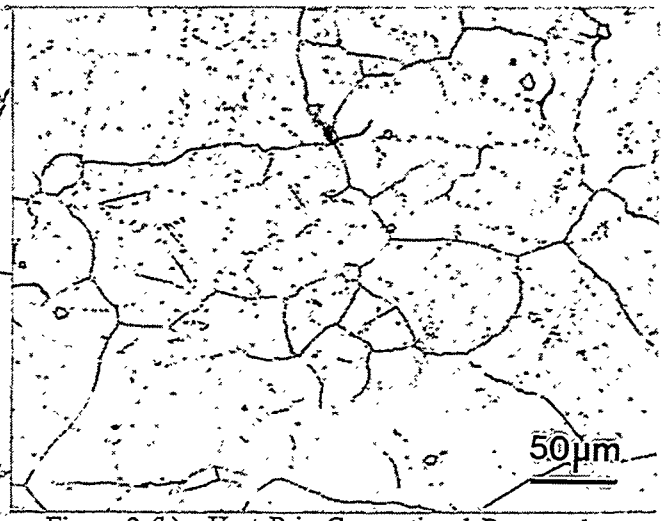

Figure 3 (b): Heat B in Conventional Processed Condition - Orthophosphoric Acid Etch

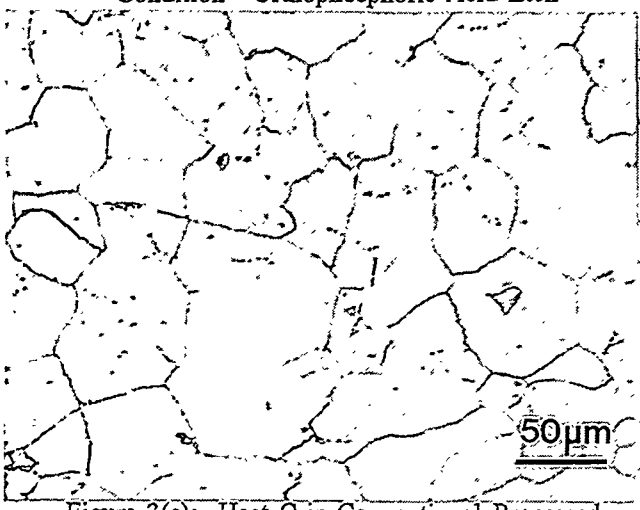

Figure 3(c): Heat C in Conventional Processed Condition - Orthophosphoric Acid Etch

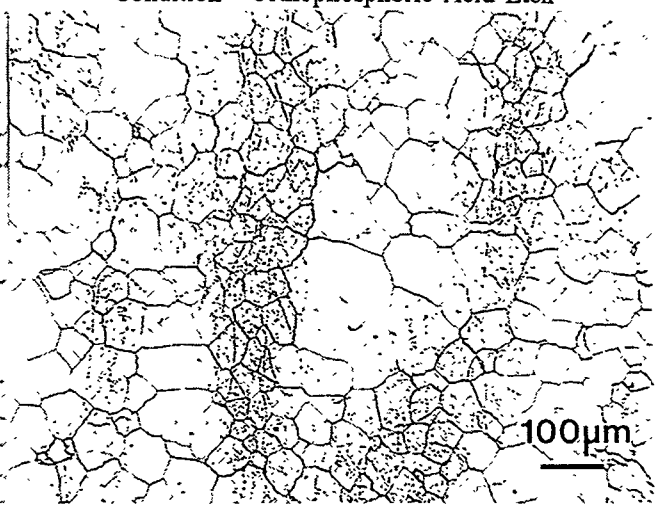

Figure 4: Example of banding in a ring rolled forging.

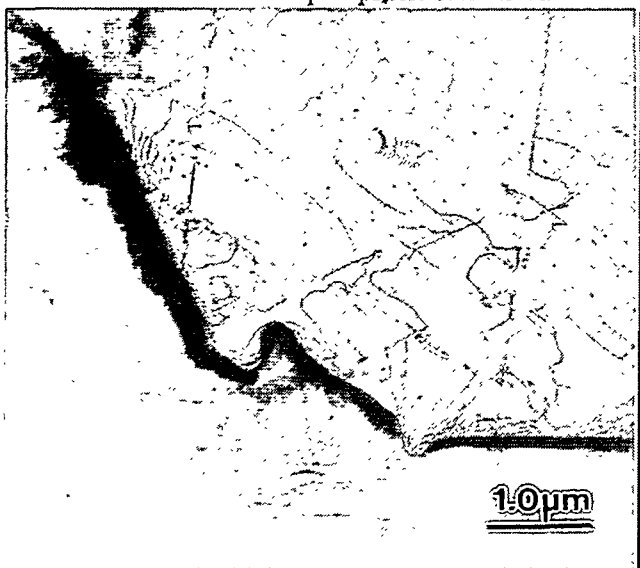

Figure 5: Transmission electron micrograph of the predominant M_7C_3 carbides observed in the forged material final-annealed at 1060°C for 2h.

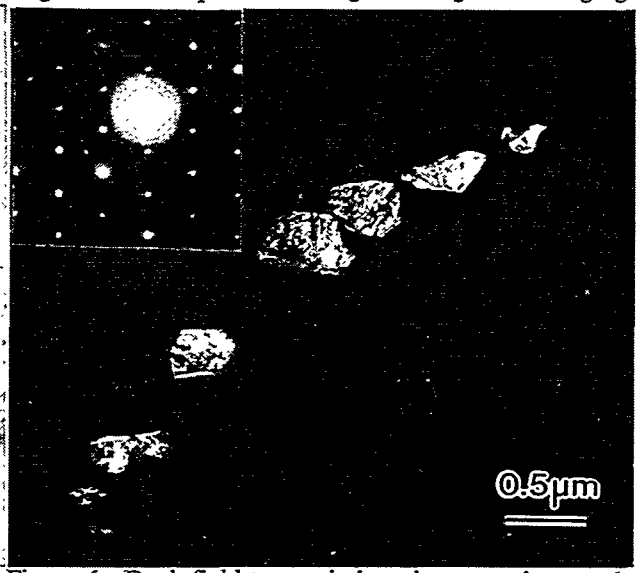

Figure 6: Dark-field transmission electron micrograph and associated selected area diffraction pattern of fine $M_{23}C_6$ carbides observed at some grain boundaries in material final-annealed at 1060°C.

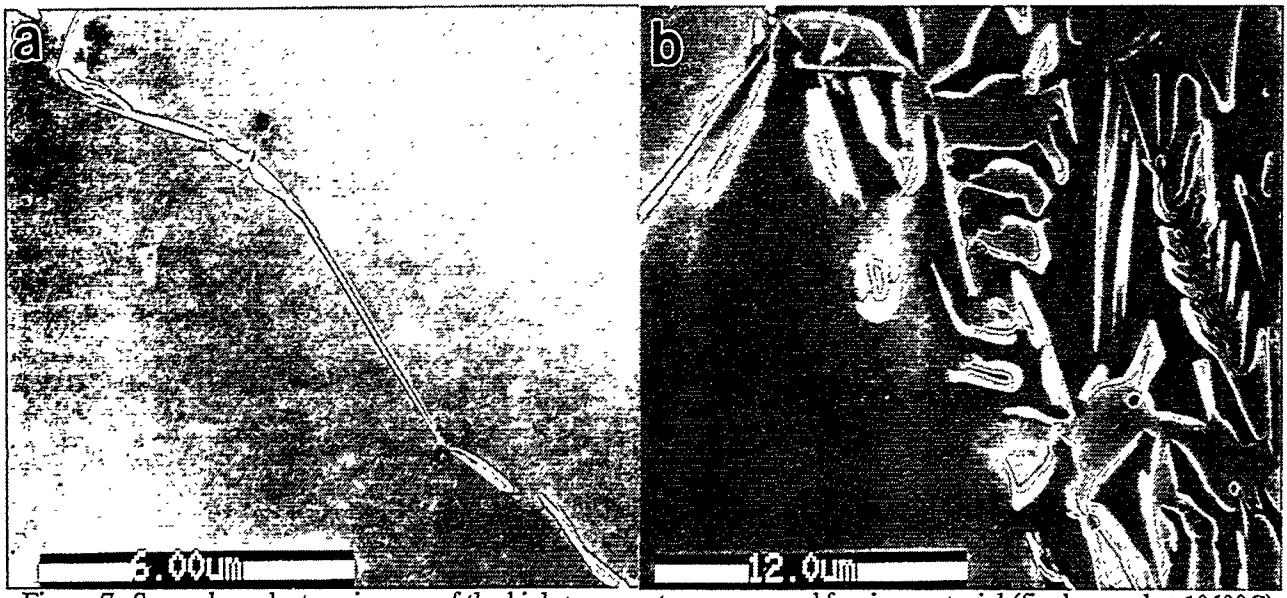

Figure 7: Secondary electron images of the high-temperature processed forging material (final anneal at 1060°C) showing the (a) "semi-continuous" and (b) dendritic-type morphologies of the M_7C_3 carbides observed.

Figure 8: Secondary electron image showing one of the few regions containing both intergranular and intragranular carbides in the material final-annealed at 1060°C for 2h.

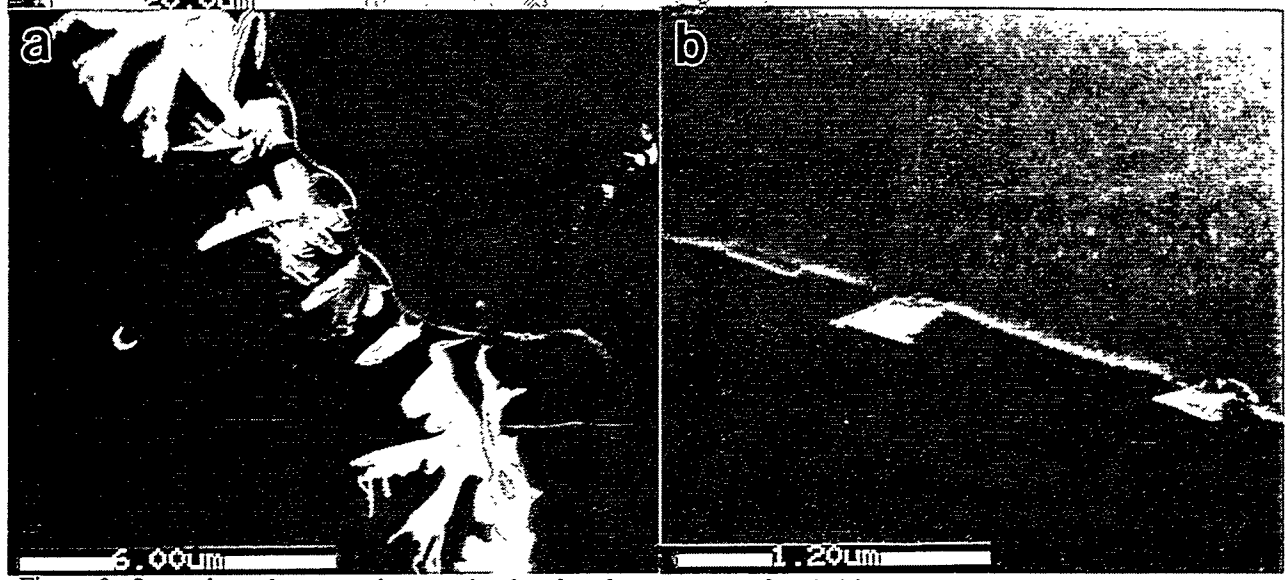

Figure 9: Secondary electron micrographs showing the presence of both (a) coarse, dendritic M_7C_3 carbides and (b) fine discrete $M_{23}C_6$ carbides in specimens final-annealed at 1024°C for 1h.

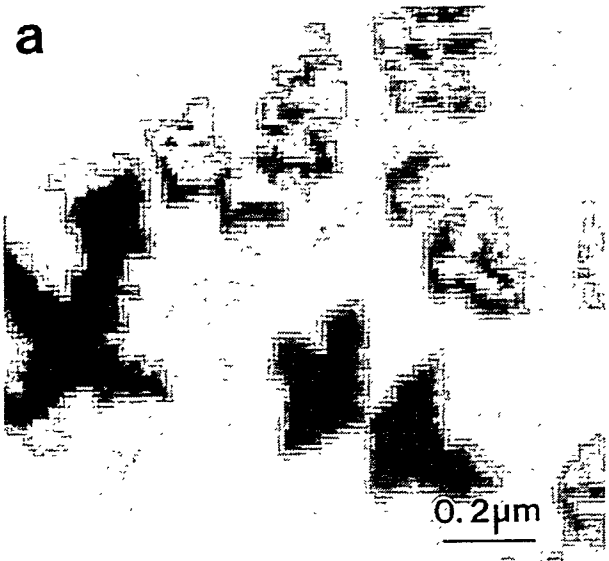

Figure 10: (a) Digitized STEM image, and corresponding x-ray maps for (b) Cr and (c) Ni which show the association of the Ni-rich precipitates with the Cr-rich carbides in material final-annealed at 1024°C for 1h.

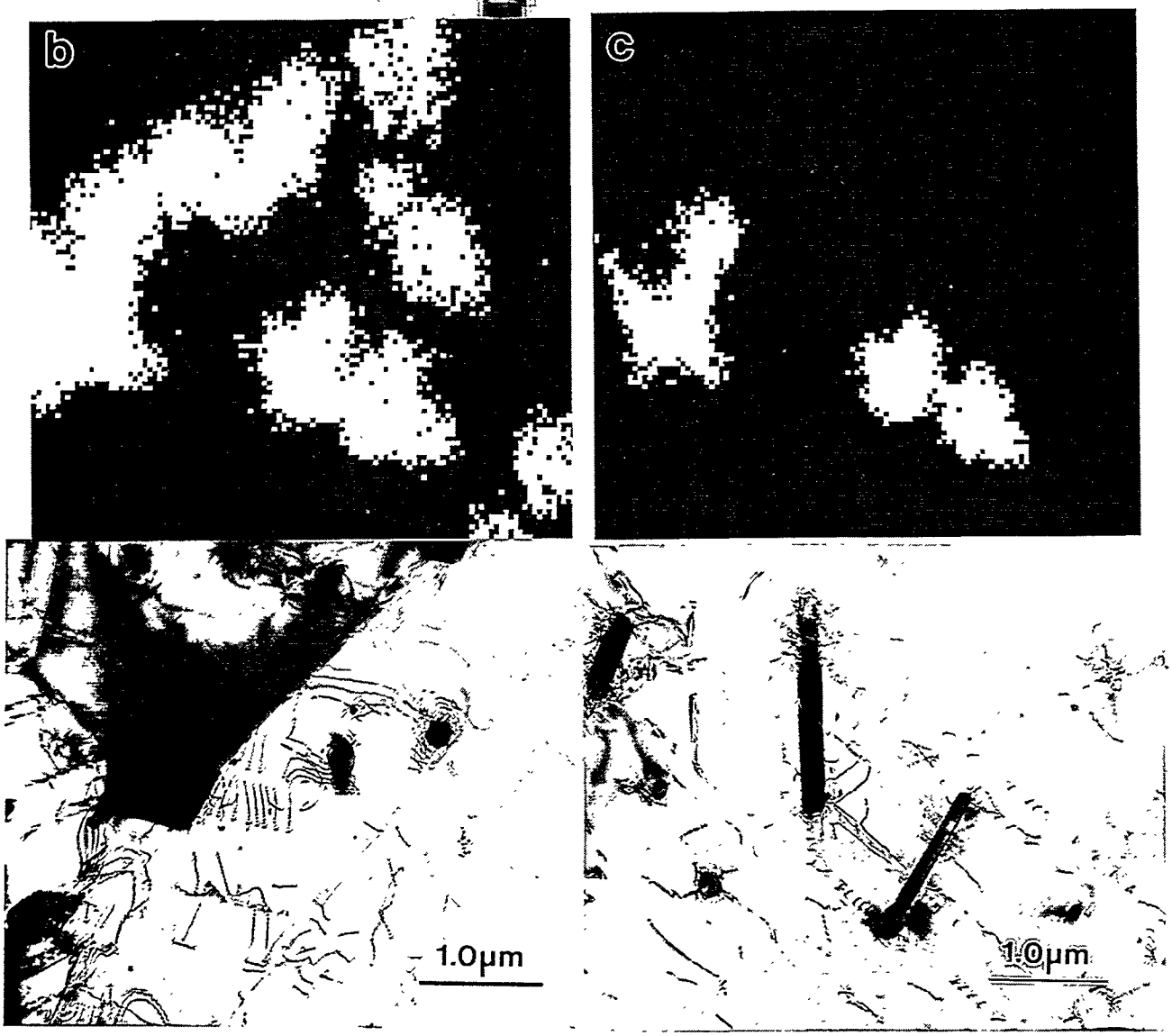

Figure 11: Transmission electron micrographs showing the two intragranular M_7C_3 carbide morphologies (globular and facetted) observed in the samples final-annealed at 1024°C for 1h.

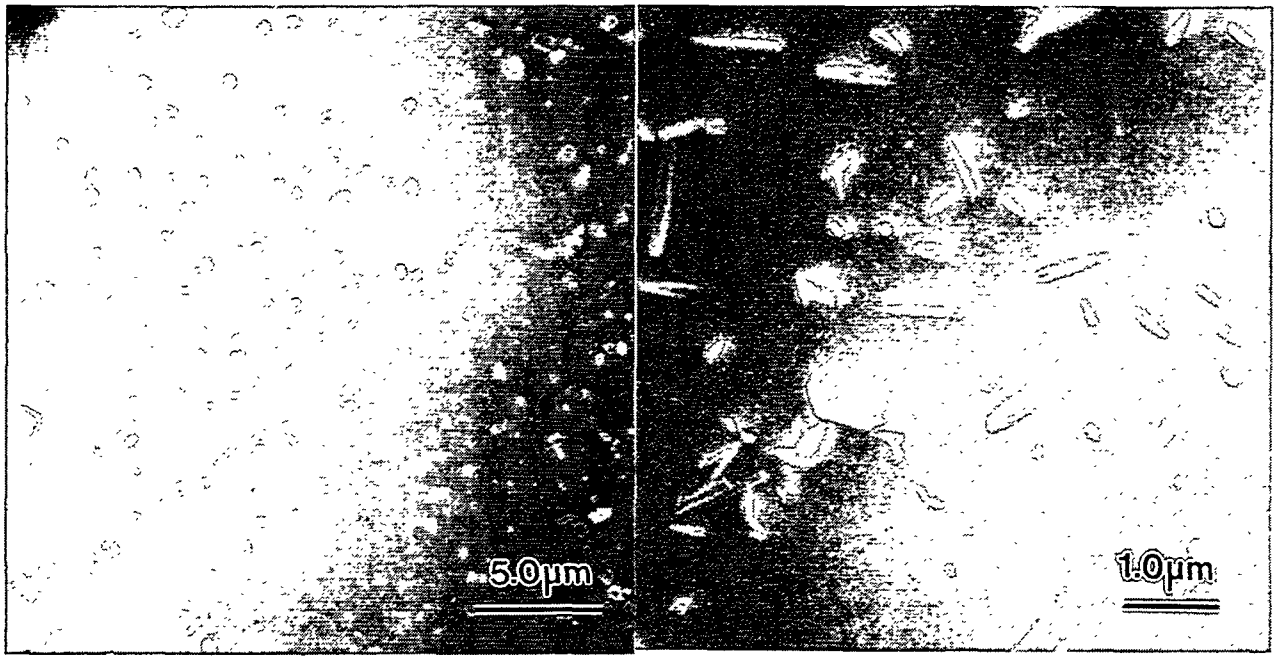

Figure 12: SEM images obtained from material final-annealed at 1024°C for 1h. Note the high proportion of intragranular M_7C_3 carbides.

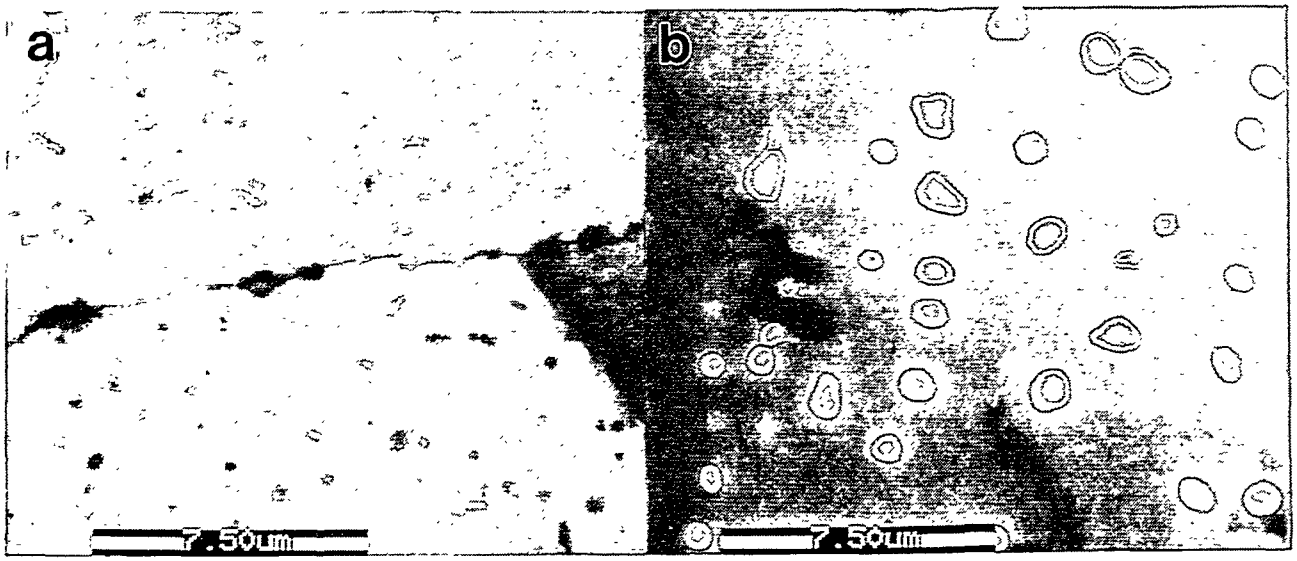

Figure 13: (a) STEM and (b) SEM images showing the extent of intergranular and intragranular carbide precipitation in conventionally-processed A600 forging with a final anneal at 1050°C for 2h.